AIAA 82-4251

Minimum Fuel Horizontal Flight Paths in the Terminal Area

Eliezer Kreindler* and Frank Neuman†
NASA Ames Research Center, Moffett Field, California

The problem of constant altitude, minimum-fuel airplane trajectories from arbitrary initial states to a fixed final state is considered. The fuel optimality of circular and straight-line flight paths is examined. Various types of representative extremals are computed and used to evaluate trajectories generated by an on-line algorithm. Attention is paid to the existence of Darboux points beyond which an extremal ceases to be globally optimal.

Nomenclature

c_0, c_1, c_2	= constants in fuel flow rate
D	= drag
g	= constant of gravity
H	= Hamiltonian
k_1, k_2	= constants in drag formula (5)
m	= mass
max	= maximal value
min	= minimal value
sgn(·)	= sign of (·)
t	= time
T	= thrust
u	= tanϕ
v	= velocity
v_c	= cruise velocity
x, y	= position coordinates
η	= multiplier for velocity constraint
λ	= costate variable
μ	= intermediate value of u, Eq. (23b)
ϕ	= bank angle
ψ	= heading angle
τ	= intermediate value of T, Eq. (20)

Subscripts

f	= final values
m	= maximum of absolute value
s	= constant values on straight-line flight
u, uu	= partial derivatives with respect to u
T	= partial derivative with respect to T

Superscripts

(·)	= time derivative
*	= optimal value

I. Introduction

THE literature on flight-path optimization is extensive. It can be classified according to paths in the vertical plane, the horizontal plane, and the three-dimensional space; it can be further classified according to the type of aircraft and mission, and the performance index. We consider minimum-fuel, constant-altitude flight paths of a transport airplane in the terminal area.

Recived July 27, 1981; revision received April 30, 1982. This paper is declared a work of the U.S. Government and therefore is in the public domain.

*NRC Associate, on leave from the Technion-Israel Institute of Technology.
†Research Scientist.

Most of the papers on flight-path optimization in the horizontal plane consider minimum time.[1-7] In Refs. 1-3, the velocity is constant; in Refs. 4-7, the velocity is a state variable as in our case, but the assumptions, constraints, and numerical results correspond to a supersonic fighter aircraft. Thus, although there is contact with our results, there is no overlap. References 8 and 9 consider minimum-fuel, horizontal rocket turns, but since the mass is variable, the results are quite different. An overview on flight-path optimization is given in Ref. 5.

Our objectives in investigating a minimum-fuel landing problem were to gain insight into the characteristics of minimum-fuel flight paths by analysis and computation, and to use these results to improve the on-line, fuel-efficient capture algorithm of Ref. 10. Details of the refined algorithm (in the horizontal plane only) are reported in Ref. 11.

Following statements of the problem and the necessary conditions in Secs. II and III, respectively, the optimality of straight-line and circular flight-path elements, which the algorithms of Refs. 10 and 11 use, is investigated in Sec. IV. It is shown that a straight-line segment can occur only at the beginning of a minimum-fuel flight path; this also revealed how such paths can be computed. Circular paths are, in general, not fuel-optimal. Computation of representative extremals is discussed in Sec. V. The resulting extremal flight paths can be grouped into three categories: 1) coasting extremals, decelerating with zero thrust throughout; 2) short-range turning extremals, where the initial and final positions, but not the headings, are relatively near (for example, 1-3 n.mi.); and 3) long-range extremals, characterized by a possible initial turn, followed by a long (for example 5-15 n.mi.) almost straight arc and ending with a possible final turn. Since the global optimality of some of these extremals was suspect, they were checked against near-optimal flight paths produced by the algorithm of Ref. 11. This comparison, discussed in Sec. VI, established the existence and approximate location of Darboux points (beyond which the extremal ceases to be globally optimal; see Ref. 12).

II. Problem Statement

The point-mass equations of motion in the horizontal plane are:

$$\dot{x} = v\cos\psi \tag{1}$$

$$\dot{y} = v\sin\psi \tag{2}$$

$$\dot{\psi} = -gu/v \tag{3}$$

$$\dot{v} = (T - D)/m \tag{4}$$

where x and y are the coordinates of the horizontal plane, ψ the heading angle measured counterclockwise from the x axis, v the velocity, g the gravitational constant, and m the mass. The control variables are the thrust T and u, where $u=\tan\phi$ and ϕ is the bank angle, positive with right wing down. The drag D is given by

$$D=k_1v^2+k_2(1+u^2)/v^2 \tag{5}$$

where k_1 and k_2 are constants (i.e., they are assumed to be independent of v for the low velocities in the terminal area). These equations were used in Refs. 4-7 and are derived by assuming zero wind velocity, constant mass, coordinated turns, and a small angle of attack which is automatically adjusted to maintain horizontal flight (see Appendix A).

Constraints and final states are:

$$|u(t)|\le u_m \tag{6}$$

$$T_{\min}\le T(t)\le T_{\max} \tag{7}$$

$$v(t)\le v_{\max} \tag{8}$$

$$x(t_f)=y(t_f)=0,\ \psi(t_f)=k2\pi,\ k=0,\pm1,\ldots,v(t_f)=v_f \tag{9}$$

The cost integral to be minimized is the fuel consumption

$$J=\int_0^{t_f}[c_0+c_1T(t)+c_2T^2(t)]\,dt, c_i=\text{const}>0,\quad i=0,1,2 \tag{10}$$

where t_f is free. The terms c_0 and c_2T^2 in the fuel flow rate are often neglected in the literature. For the case considered here, c_0, the fuel flow rate at zero thrust, is not negligible. The term c_2T^2 is small but significant: when $c_2=0$, the optimal thrust is discontinuous and its intermediate values are singular (see Appendix B). By changing the units of c_i, the cost integal J can be interpreted as a combination of the cost of time and fuel (the operating cost). The time-optimal problem, $c_0=1$, $c_1=c_2=0$, has been treated in Refs. 1-7 and is not considered here.

In summary, the problem is to determine controls $u(t)$ and $T(t)$ and the corresponding state trajectory from an arbitrary initial state at time $t=0$ to the final state of Eq. (9) at a free time $t=t_f$, subject to Eqs. (1-8), in order to minimize fuel consumption [Eq. (10)].

For our general analysis, we make the following two assumptions, which are easily satisifed for our (and indeed for most) numerical values.

Assumption 1: For the applicable range of velocities, the thrust that equals drag is intermediate. This implies that the two velocities for which $T_{\max}=D$ are outside the applicable range. It also implies that $T_{\min}$ is less than the minimal drag with respect to velocity, $D_{\min}$. In the general case, $T_{\min}$ can be negative, and we make Assumption 2.

Assumption 2: $T_{\min}$ is such that the fuel flow rate at $T=T_{\min}$ is positive and $T_{\min}>-c_1/(2c_2)$. The first part eliminates consideration of gliding flight paths with shut-off engines; all such paths are fuel-optimal and trivially satisfy the necessary conditions embodied in the minimum principle. The significance of the second part is discussed in the next section.

Numerical values used in this study correspond to a 150,000-lb jet transport at sea level at velocities not below 150 knots.

$v_{\max}=250$ knots, $v_f=180$ knots

$T_{\max}=30{,}000$ lb, $T_{\min}=0$

$\phi_m=30$ deg, $\tan\phi_m=u_m=0.577$

$k_1=0.08$ lb/knot^2, $k_2=2.127\times10^8$ lb knot^2

$c_0=0.808$ lb s^{-1}, $c_1=1.507\times10^{-4}$ s^{-1},

$c_2=5.4\times10^{-10}$ lb^{-1} s^{-1}

To get an idea of the percentage contributions of the terms c_0, c_1T, and c_2T^2 in Eq. (10) to the total fuel flow rate, assume a flight along a straight line at a constant velocity of 250 knots (at $T=D=8403$ lb). The contributions are then 38% for c_0, 60% for c_1T, and 2% for c_2T^2. Assumption 1 is easily satisfied: we find that $T_{\max}=D$ occurs at 83 knots and 607 knots, and that $D_{\min}$ is 8250 lb at 227 knots. Evidently, Assumption 2 is also satisified.

III. Necessary Conditions

We employ the minimum principle. The Hamiltonian is:

$$H=\lambda_0(c_0+c_1T+c_2T^2)+\lambda_x v\cos\psi+\lambda_y v\sin\psi-\lambda_\psi gu/v$$
$$+\lambda_v[T-k_1v^2-k_2(1+u^2)/v^2]/m+\eta(v-v_{\max}) \tag{11}$$

where $\eta\ge0$, $\eta(v-v_{\max})\equiv0$ (Ref. 13). The costate variables are given by

$$\lambda_0\ge0,\qquad \lambda_0=\text{const} \tag{12}$$

$$\dot\lambda_x=-H_x=0\Rightarrow\lambda_x=\text{const} \tag{13}$$

$$\dot\lambda_y=-H_y=0\Rightarrow\lambda_y=\text{const} \tag{14}$$

$$\dot\lambda_\psi=-H_\psi=v(\lambda_x\sin\psi-\lambda_y\cos\psi) \tag{15}$$

$$\dot\lambda_v=-H_v=-\lambda_x\cos\psi-\lambda_y\sin\psi-\lambda_\psi gu/v^2$$
$$+2\lambda_v[k_1v-k_2(1+u^2)/v^3]/m-\eta \tag{16}$$

where $H_x=\partial H/\partial x$, etc. Since t_f is not prescribed and $H_t=0$, we have the necessary condition

$$H\equiv0,\qquad \text{all}\quad t\in[0,t_f] \tag{17}$$

If for some t,

$$\lambda_\psi(t)=\lambda_v(t)=0=\lambda_x=\lambda_y \tag{18}$$

then Eq. (17) and Assumption 2 require the vanishing of λ_0. Since having all costates zero is not optimal, an extremal where Eq. (18) occurs is not fuel-optimal. Henceforth, we consider only extremals with $\lambda_0>0$, and we normalize the costates by setting $\lambda_0=1$.

Minimization of H with respect to T yields the extremal thrust

$$T^*=\begin{cases}T_{\max} & \text{if}\quad \tau\ge T_{\max}\\ \tau & \text{if}\quad T_{\min}<\tau<T_{\max}\\ T_{\min} & \text{if}\quad \tau\le T_{\min}\end{cases} \tag{19}$$

where

$$\tau=\frac{-(c_1+\lambda_v/m)}{2c_2} \tag{20}$$

We note that by Assumption 2, Eqs. (19) and (20) show at once that

$$T^* = T_{\min} \quad \text{if} \quad \lambda_v \geq 0 \tag{21}$$

Since the minimization of H yields T^* uniquely, it can be shown (see Ref. 13) that T^* and λ_v are continuous at junction times between the velocity-constrained and the unconstrained arcs. Thus thrust is seen to be a continuous function of λ_v and t. When c_2 is small, the range of λ_v for intermediate thrust is narrow; when $c_2 = 0$, the intermediate thrust is singular. (In some cases, not considered in this paper, c_2 is negative; then, intermediate thrust is not fuel-optimal.)

We observe that Eqs. (3) and (15) for ψ and λ_ψ, respectively, and the fact that λ_x and λ_y are constant, imply

$$u \equiv 0 \quad \text{if} \quad \lambda_\psi \equiv 0 \quad \text{on an interval} \tag{22}$$

This is true irrespective of the minimization of H with respect to u. From the latter, we obtain, by using $H_u = 0$ and $H_{uu} > 0$,

$$u^* = \begin{cases} \mu & \text{if } |\mu| < u_m \quad \text{and} \quad \lambda_v < 0 \\ u_m \operatorname{sgn}\mu = u_m \operatorname{sgn}\lambda_\psi & \text{if } |\mu| \geq u_m \quad \text{and } \lambda_v < 0 \end{cases} \tag{23a}$$

where

$$\mu = -gmv\lambda_\psi / 2k_2\lambda_v \tag{23b}$$

If $\lambda_v \geq 0$ and λ_ψ does not vanish on an interval (denoted by $\lambda_\psi \not\equiv 0$), the minimization of H gives at once

$$u^* = -u_m \operatorname{sgn}\lambda_\psi \quad \text{if} \quad \lambda_v \geq 0 \quad \text{and} \quad \lambda_\psi \not\equiv 0 \tag{23c}$$

We note that λ_v cannot be positive while λ_ψ vanishes on an interval because minimization of H then implies $u^* = \pm u_m$, which is incompatible with Eq. (22). However, if λ_ψ vanishes on an interval and λ_v crosses zero from negative to positive values, say at $t = t_2$, then u switches from $u(t) = 0$, $t \leq t_2$ to $u(t_2^+) = \pm u_m$; this is a transition from a straight-line flight path to a curved one.

We also note that the simultaneous vanishing on an interval of λ_ψ and λ_v is not fuel-optimal because it implies the vanishing of $\dot{\lambda}_\psi$ and $\dot{\lambda}_v$, which in turn implies $\lambda_x = \lambda_y = 0$, that is, the nonoptimal case of Eq. (18).

In summary, we see that u, and hence the bank angle, are continuous in time when λ_v is negative; u is discontinuous when λ_v is positive, or at the moment λ_v crosses zero to become positive and λ_ψ had been zero on the previous interval. In view of Eq. (21), discontinuity of the bank angle occurs at minimum thrust.

Lastly, we evaluate η. When $v(t) \equiv v_{\max}$, the thrust is intermediate under Assumption 1. Then, by Eqs. (5) and (20), $T = D$ gives

$$-(c_1 + \lambda_v/m)/2c_2 = k_1 v_{\max}^2 + k_2/v_{\max}^2 + k_2 u^2/v_{\max}^2$$

This equation gives an expression for λ_v and, upon differentiation, for $\dot{\lambda}_v$, which we substitute into Eq. (16) to obtain

$$\eta = -\lambda_x \cos\psi - \lambda_y \sin\psi - \lambda_\psi g u / v_{\max}^2 + 4mc_2 k_2 u\dot{u}/v_{\max}^2$$
$$-2\{c_1 + 2c_2[k_1 v_{\max}^2 + k_2(1+u^2)/v_{\max}^2]\}[k_1 v_{\max}$$
$$-k_2(1+u^2)/v_{\max}^3] \tag{24}$$

For a velocity-constrained arc to be optimal, $\eta(t)$, given by Eq. (24), must be nonnegative.

IV. Optimality of Straight-Line and Circular Path Elements

Since the suboptimal algorithms of Refs. 10 and 11 are based on piecing together circular arcs and, at most, one straight-line segment, we are interested in the optimality of these path elements.

We first show that *there can be at most one straight-line segment in a fuel-optimal path and, if it occurs, it must do so at the beginning of the path. A subsequent curved path, if any, starts by a switch to maximum bank angle* $|\phi| = \phi_m$ *at (continuous) minimum thrust* $T = T_{\min}$; *the bank angle's magnitude and the thrust remain at* ϕ_m and $T_{\min}$, *respectively, as long as* λ_v *remains positive.*

To prove this proposition, we note that flight along a straight-line segment on a subinterval $[t_1, t_2]$ is characterized by

$$\psi(t) = \psi_s, \quad u(t) = 0 = \lambda_\psi(t), \quad \lambda_v(t) < 0, \quad \text{on} \quad [t_1, t_2] \tag{25}$$

We observe that for a straight-line path, the point ($\psi = \psi_s$, $\lambda_\psi = 0$) is an equilibrium point‡ for Eqs. (3) and (15) for $\dot{\psi}$ and $\dot{\lambda}_\psi$, with $v(t)$ as a continuous parameter. Hence the straight-line segment can be entered at t_1 and exited at t_2 by an optimal control only if the control is discontinuous at t_1 and t_2. Therefore, as noted in the discussion following Eq. (24), it is necessary that $\lambda_v(t)$ cross zero at t_1 and t_2 according to

$$\lambda_v(t_1) = 0, \qquad \dot{\lambda}_v(t_1) < 0 \tag{26}$$

and

$$\lambda_v(t_2) = 0, \qquad \dot{\lambda}_v(t_2) > 0 \tag{27}$$

(This causes $u(t)$ to switch from $u(t_1^-) = \pm u_m$ to $u(t) = 0$ on $[t_1, t_2]$ and back to $u(t_2^+) = \pm u_m$.) Thus, $\lambda_v(t_i) = 0$, $i = 1, 2$; by Eq. (21) this implies $T(t_i) = T_{\min}$. Using

$$\lambda_\psi(t_i) = \lambda_v(t_i) = 0 \tag{28}$$

in Eq. (17) gives

$$\dot{f}_{\min} = -v(t_i)(\lambda_x \cos\psi_s + \lambda_y \sin\psi_s) \tag{29}$$

Equation (29) together with $\dot{\lambda}_{\psi}(t_i)$ in Eq. (15) gives

$$\lambda_x = \frac{-\dot{f}_{\min}\cos\psi_s}{v(t_i)} \qquad i = 1,2 \tag{30}$$

and

$$\lambda_y = \frac{-\dot{f}_{\min}\sin\psi_s}{v(t_i)} \qquad i = 1,2 \tag{31}$$

where $\dot{f}_{\min}$ is the fuel flow rate at $T_{\min}$

$$\dot{f}_{\min} = c_0 + c_1 T_{\min} + c_2 T_{\min}^2 \tag{32}$$

Using Eqs. (28-32) in Eq. (16) gives

$$\dot{\lambda}_v(t_i) = \frac{\dot{f}_{\min}}{v(t_i)} \qquad i = 1,2 \tag{33}$$

Since by Assumption 2 $\dot{f}_{\min}$ is positive, Eq. (33) shows that $\dot{\lambda}_v(t_i) > 0$, $i = 1,2$. This contradicts Eq. (26) but confirms Eq. (27). Hence a curved flight path cannot precede but can follow

‡An equilibrium point of the differential equation $\dot{x} = f(x,t)$ is a point x_e that satisfies $0 = f(x_e, t)$. By uniqueness, a solution $x(t)$ started outside (at) the equilibrium point cannot reach it (depart from it) in finite time (see, e.g., Ref. 14, p, 276).

a straight-line segment. On the curved path, at least initially, $\lambda_v(t) > 0$, $t > t_2$. Hence, by Eq. (23c), $|u(t)| = u_m$, and by Eq. (21), $T = T_{\min}$. This completes the proof.

Next, we ask whether cruise at a constant velocity $v(t) \equiv v_c < v_{\max}$ on a straight-line segment is fuel-optimal. For the purpose of the inquiry, we temporarily lift the constraint $v(t) \le v_{\max}$. We find that *a flight at constant velocity on a straight-line segment of a flight path can be fuel-optimal only if the entire flight path is straight, flown at a constant optimal cruise velocity* v_c^* *given by the solution of the equation*

$$3c_2k_1^2v_c^8 + c_1k_1v_c^6 - (c_0 + 2c_2k_1k_2)v_c^4 - 3c_1k_2v_c^2 - 5c_2k_2 = 0 \tag{34}$$

Equation (34) *has one and only one real and positive solution.*

Proof: For flight on a straight path at a constant velocity v_c, the thrust is constant, $T = T_c = D(v_c)$, and, by Assumption 1, is intermediate; hence, λ_v must be constant, $\lambda_v = \lambda_{v_c}$, according to Eq. (20). The point ($\psi = \psi_s$, $v = v_c$, $\lambda_\psi = 0$, $\lambda_v = \lambda_{v_c}$) is an equilibrium point for the respective set of differential equations [Eqs. (3), (9), (15), and (16)], whence follows the first part of the proposition. To derive Eq. (34), we eliminate λ_x and λ_y in Eq. (16) by using Eq. (17), and we substitute the value of $\lambda_v = \lambda_{v_c}$ from Eq. (20). This yields

$$\dot{\lambda}_v v_c = \{c_0 + c_1(k_1v_c^2 + k_2/v_c^2) + c_2(k_1v_c^2 + k_2/v_c^2)^2 - 2[2c_2(k_1v_c^2 + k_2/v_c^2) + c_1](k_1v_c^2 - k_2/v_c^2)\} \tag{35}$$

Since λ_v is a constant, the right side of Eq. (35) vanishes, yielding Eq. (34). Let the right side of Eq. (35) be denoted by $f(v_c)$. Then

$$df(v_c)/dv_c = -2(c_1k_1v_c + 3c_2k_2/v_c^3 + 6c_2k_1^2v_c^3 + 10c_2k_2^2/v_c^5) \tag{36}$$

For sufficiently small v_c, $f(v_c) > 0$, and from Eq. (36), $df/dv_c < 0$ for all positive v_c. Hence, $f(v_c)$ is monotonically decreasing and has one and only one real and positive zero $v_c = v_c^*$. This completes the proof.

The significance of the velocity v_c^* is that *when the entire flight path is straight,* v_c^* *is an upper bound on* $v(t)$, $t \in [0, t_f]$ in the sense

$$\text{if } v(0) < v_c^* \text{ and } v_f < v_c^*, \text{ then } v(t) < v_c^* \tag{37}$$

and a lower bound in the sense

$$\text{if } v(0) > v_c^* \text{ and } v_f > v_c^*, \text{ then } v(t) > v_c^* \tag{38}$$

Proof: Consider Eq. (37), and suppose that the velocity rises to a maximum $v(t') \ge v^*$; there $\dot{v}(t') = 0$, and $\ddot{v}(t') < 0$ which we want to contradict. At $t = t'$ we have

$$\ddot{v}(t') = [\dot{T} - (dD/dv)\dot{v}(t')]/m = \dot{T}/m = -2c_1\dot{\lambda}_v(t')/m^2 \tag{39}$$

Since $\dot{v}(t') = 0$, Eq. (35) applies with $v(t')$ replacing v_c. For $v(t') = v_c^*$, the left side of Eq. (35) vanishes. Since by Eq. (36) the right side of Eq. (35) is decreasing, then, if $v(t') \ge v_c^*$, we have $\dot{\lambda}_v(t') \le 0$. It follows from Eq. (39) that $\ddot{v}(t') \ge 0$, which is a contradiction. This proves Eq. (37); Eq. (38) is proved analogously. We note in passing that by linearizing the equations for v and λ_v around the equilibrium point (v_c^*, λ_{v_c}), this point can be shown to be a saddle point, which conforms with Eqs. (37) and (38).

The case of Eq. (38) is of little interest for landing because usually $v_f < v_c^*$. If $v(0)$ and v_f are on opposite sides of v_c^*, then $v(t)$ can cross v_c^*. Our numerical experience, described in the next section, shows that v_c^* acts as an upper bound on $v(t)$ also for relatively long-range flight paths which are not strictly straight. Considering now the constraint $v(t) \le v_{\max}$ for the case of Eq. (37), it is clear that it will be inactive if $v_{\max} \ge v_c^*$ and is likely to be active if $v_{\max}$ is much below v_c^*.

The optimal cruise velocity v_c^*, given by Eq. (34), is the velocity that provides minimum fuel consumption per unit distance along a straight flight path. One expects that v_c^* will be higher if $c_2 = 0$ in the fuel consumption model of Eq. (10), and will be lower if $c_0 = 0$. For our numerical values,

$$v_c^* = \begin{cases} 349.5 \text{ knots} & \text{if } c_0 \neq 0, \quad c_2 \neq 0 \\ 359.0 \text{ knots} & \text{if } c_0 \neq 0, \quad c_2 = 0 \\ 298.8 \text{ knots} & \text{if } c_0 = 0, \quad c_2 = 0 \end{cases}$$

For comparison, the minimum drag velocity, which is the minimum fuel per unit time velocity, is

$$v_{D_{\min}} = (k_2/k_1)^{1/4} = 227 \text{ knots}$$

Examination of the necessary conditions shows that a circular flight path can be fuel-optimal only if both the bank angle and the velocity are at their respective constraint bounds. The proof is straightforward and is omitted.

V. Computation of Extremals

The extremals are computed by numerical integration of the state and costate equations [Eqs. (1-5) and (12-16)], with the controls given by Eqs. (19) and (23) from a given state, and with chosen initial values of the costate variables as parameters. One can thus obtain families of extremals but cannot meet specified end conditions.

In the computations, the state constraint $v \le v_{\max} = 250$ knots was imposed only on some of the long-range flight paths; however, no extremal was extended beyond 350 knots. A state constraint $v \ge v_{\min}$ was not explicitly incorporated in the necessary conditions; however, extremals where $v(t)$ dropped below 150 knots were rejected because the drag model of Eq. (5) would not be valid below that velocity.

In the following figures, distances are in nautical miles, velocities v in knots, thrust T in thousands of pounds, fuel consumption f to the final point in pounds, and time in seconds is from the integration's starting time $t_s = 0$. The portions of the flight path with $T > 0$ are in bold curves. The maximal and minimal values of thrust and velocity are among the T's and v's shown. The arrows show the airplane's direction of flight. The starting values of the costates at $t_s = 0$ are shown in the figures by

$$\lambda_y' = \lambda_y/c_1, \qquad \lambda_\psi' = \lambda_\psi/c_1, \quad \lambda_v' = \lambda_v/c_1 m$$

(In our computations we divided the Hamiltonian by c_1.)

It is convenient to start integration backwards from the known and fixed final state of Eq. (9). Computing λ_x from the condition $H = 0$ at the integration's starting time t_s, the extremals are determined by the parameters λ_y, $\lambda_\psi(t_s)$, and $\lambda_v(t_s)$. Since the problem is time-invariant, we set $t_s = 0$. The sign and relative magntiude of both λ_y and $\lambda_\psi(t_f)$ determine the direction of turn; it can be shown that by changing the sign of both, the flight path is reflected about the x axis (true if integration is started at $y = \psi = 0$). Such backward integration produced coasting and short-range turning extremals, as those shown in Figs. 1 and 2.

Figure 1 shows coasting flight paths, namely, decelerating paths with zero thrust throughout. For extremals 1 and 2, the bank angle switches between its bounds of ± 30 deg because $\lambda_v(t)$ is positive throughout. This is typical of most, but not all, coasting extremals; extremal 3 ends with a smooth transition to a shallow bank angle, and extremal 4 starts with a straight-line segment. Coasting extemals may be significant for emergency landing.

Figure 2 shows (by solid curves) partly thrusting extremal paths whose backward computation was arbitrarily ter-

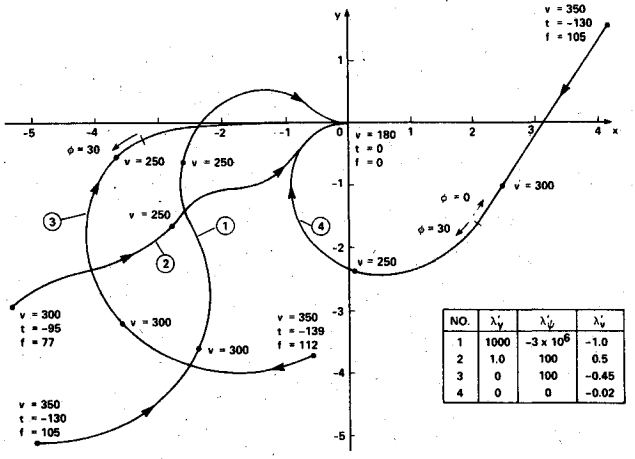

NO.	λ_y'	λ_ψ'	λ_v'
1	1000	-3×10^6	-1.0
2	1.0	100	0.5
3	0	100	-0.45
4	0	0	-0.02

Fig. 1 Coasting (zero-thrust) flight paths.

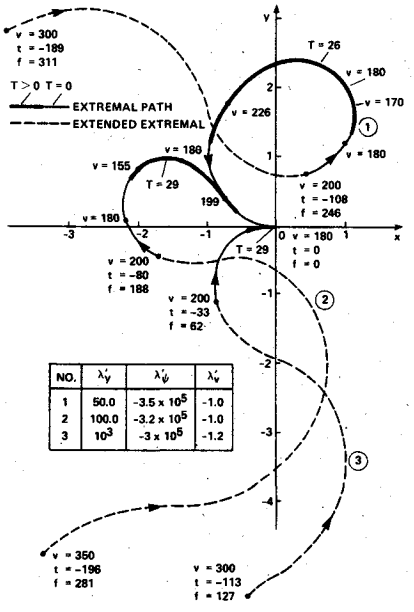

NO.	λ_y'	λ_ψ'	λ_v'
1	50.0	-3.5×10^5	-1.0
2	100.0	-3.2×10^5	-1.0
3	10^3	-3×10^5	-1.2

Fig. 2 Short-range turning flight paths.

minated at 200 knots. These paths represent short-range turning approaches starting at 200 knots, such as after an aborted landing. Typically, for a turn through a large angle, as in paths 1 and 2, the velocity first drops to achieve a tighter turn. This was noted in Ref. 6 for minimum-time turns, but is less intuitively obvious in the minimum-fuel case because fuel is later expended to accelerate. The broken curves, here and in Fig. 4, will be commented on in the next section.

Backward integration from the final state did not produce long-range flight paths. Such paths require a sustained intermediate thrust which is dictated by a narrow range of λ_v [from Eq. (20) it follows at once that $T \geq T_{\min} = 0$ if $\lambda_v/c_1 m \geq -1.0$, and by computation, $T \leq T_{\max}$ if $\lambda_v/c_1 m \leq -1.215$], resulting in extreme sensitivity to the choice of $\lambda_v(t_s)$. Therefore, long-range extremals, and other types of extremals with special conditions at intermediate points, were produced by forward and backward integration from an appropriate intermediate state. For convenience, integration was started at $x(t_s) = y(t_s) = \psi(t_s) = 0$, $t_s = 0$, with an appropriate $v(t_s)$. The resulting flight path can then be shifted and rotated to satisfy the final condition of Eq. (9).

Integration of long-range extremals without the velocity constraint [Eq. (8)] was started at a velocity below the optimal cruise veloicy $v_c^* = 349.5$, with λ_v such that $T = D$. The parameters are then $v(t_s)$, λ_y and $\lambda_\psi(t_s)$, $t_s = 0$. The velocity profiles of such paths are shown in Fig. 3. Since $\dot{v}(t_s) = 0$,

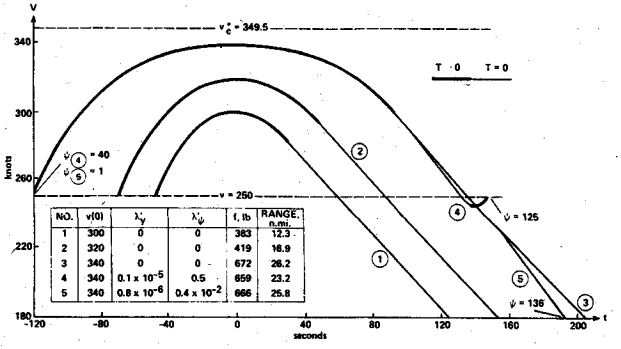

NO.	v(0)	λ_y'	λ_ψ'	f, lb	RANGE, n.mi.
1	300	0	0	383	12.3
2	320	0	0	419	16.9
3	340	0	0	672	26.2
4	340	0.1×10^{-5}	0.5	659	23.2
5	340	0.8×10^{-6}	0.4×10^{-2}	666	25.8

Fig. 3 Velocity profiles for long-range flight paths without a velocity constraint.

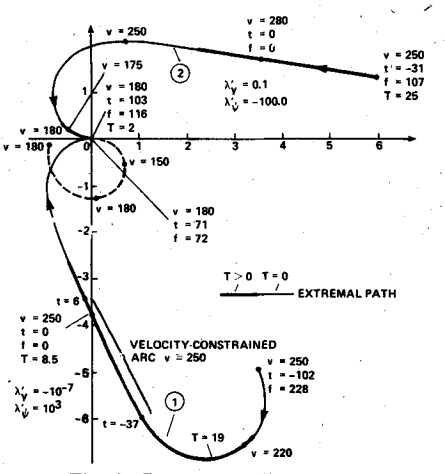

Fig. 4 Long-range flight paths.

$v(t_s)$ is the maximal velocity. Curves 1-3 correspond to straight-line flight paths. Curves 4 and 5 correspond to paths with initial and final turns as indicated. For $t < 0$, curves 3, 4, and 5 are indistinguishable. On curve 4, we note the dip in velocity at the large final turn to $v(t_f) = 250$ knots. On curve 5 the velocity decreases faster than on curve 3 because of the added drag due to maximum bank angle.

Extremals with a velocity-constrained arc were computed by starting on the arc at $v(t_s) = v_{\max} = 250$ knots. The costate $\lambda_v(t_s)$ is determined by the requirement that thrust equal drag. The remaining parameters are λ_y, $\lambda_\psi(t_s)$, and two parameters to control the departures from the velocity-constrained arc according to preset times or according to the multiplier $\eta(t) \geq 0$ computed by Eq. (24). We considered extremals with only one constrained arc of the long-range type.

Figure 4 shows long-range flight paths, which typically consist of a possible initial turn, a long, almost straight arc, and a possible final turn. Path 1 is a velocity-constrained extremal, path 2 is unconstrained, and both were computed from the point indicated by $t = 0$. For convenience of presentation, neither path is particularly long. In both cases the almost straight arc can be made as long as desired: in the constrained case by selecting λ_y and $\lambda_\psi(0)$ sufficiently small, and in the unconstrained case by selecting, in addition, $v(0)$ sufficiently close to the optimal cruise velocity v_c^*.

Integration from an intermediate state, rather than from an end state, is mandatory also for the type of extremal discussed in Sec. IV: a straight-line segment followed by a switch to a maximal bank angle turn. This extremal requires the satisfaction of Eq. (33) at the switch time t_2. Since $\psi(t)$, $u(t)$, $\lambda_\psi(t)$, and λ_y are zero on the straight-line segment, the remaining parameters are $v(t_s)$ and $\lambda_v(t_s) < 0$. For our numerical values and range of velocity, these extremals (such as flight path 4 in Fig. 1 whose integration started at the point

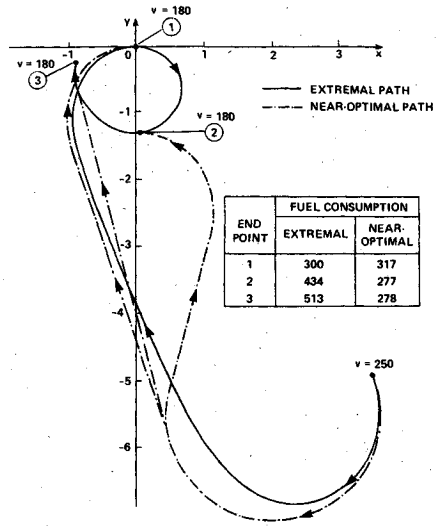

END POINT	FUEL CONSUMPTION	
	EXTREMAL	NEAR-OPTIMAL
1	300	317
2	434	277
3	513	278

a)

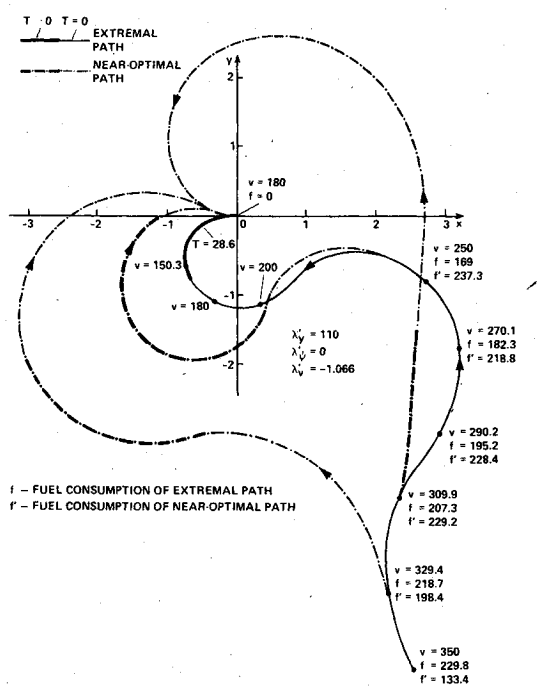

b)

Fig. 5 Comparison of extremal and near-optimal flight paths: a) long-range paths; b) short-range turning paths.

indicated by $v=300$ knots) are all coasting extremals with maximal bank angle throughout the turn.

The accuracy of the computed extremals was checked by decreasing the integration step and by observing the accuracy of the condition $H=0$.

VI. Optimal and Near-Optimal Solutions

We now compare the fuel consumption of flight paths produced by extremals with that of near-optimal paths. We thus test the quality of the near-optimal paths as well as the global optimality of the extremals.

The near-optimal algorithm of Ref. 10 generates a flyable state trajectory between any two end states; it is sufficiently fast to be operated onboard and in real time. The algorithm, based on the results in Ref. 1, generates the shortest flyable path consisting of circular paths joined by, at most, one straight-line segment. In Ref. 11, the algorithm is further refined in light of the results of this study; in particular, the curved path is created by a succession of 30-deg circular arcs of varying radii. In view of the results of Sec. III, it is clear that such a synthesized flight path cannot be fuel-optimal. However, it is evident from Fig. 4 that such paths can closely approximate the optimal ones for the most common and important type of path, the long-range path. The details of the algorithm as well as numerous comparisons are reported in Ref. 11. For example, for 28 long-range paths of about 20 miles, without a velocity constraint, the worst approximation was 2.95% off the minimum fuel consumption, the best 0.5%, and the average 1.52% (Ref. 11).

The extremals exhibited in Sec. V satisfy only necessary conditions for optimality. Are they optimal? We have no proof, but fuel optimality can be argued for at least the coasting extremals, which are also minimum-time coasting extremals. Consider flight paths 1 and 2 in Fig. 1. Along these the magnitude of the bank angle, and hence the drag, are maximal at all times. Therefore, any other coasting flight path with $x(t_f')=y(t_f')=\psi(t_f')=0$, $t_f'<t_f$, must have $v(t_f')>v_f=180$ knots. The fuel optimality of paths 3 and 4 can be supported by similar, albeit somewhat weaker, arguments.

The situation is far less clear for the thrusting extremals. These, as the integration continued, often started twisting and looping in a manner which appears increasingly nonoptimal, as shown by the broken curves of Figs. 2 and 4. Such behavior of extremals is likely to have been observed previously; there is an allusion to loss of global optimality in Ref. 7. In general, as an extremal is extended by integration from some starting point, a time t_D may be reached beyond which the etremal ceases to be globally optimal; t_D is called a *Darboux point* with respect to the starting point.[12]

The existence of Darboux points on the extremals of Figs. 2 and 4 is demonstrated in Fig. 5 by comparison of fuel consumption with near-optimal paths. Figure 5a shows path 1 of Fig. 4 which, as the forward integration is extended, has in the final turn three points with $v=180$ knots. The comparison confirms the nonoptimality of end points 2 and 3; the Darboux point appears to be about midway between points 1 and 2. We note that path 2 of Fig. 4 also has two possible end points with $v=180$ knots. In this case, however, the extremal path to the second end point is deemed to be optimal. Figure 5b shows the fuel consumption to the final point $x=y=0$ of a turning extremal path and of near-optimal paths, for several points along the extremal; three such near-optimal paths are shown. Evidently, for points beyond $v=320$ knots or so, the near-optimal paths use less fuel. Although we do not have the exact location of the Darboux point, we are confident that if the extremal is terminated at, say, 250 knots, it is optimal.

Thus, although one cannot use the near-optimal paths to prove optimality, one can get a rough idea of the location of the Darboux point, particularly for the long-range paths where the near-optimal approximation is very good. Of course, portions of nonoptimal extremals may be optimal; for example, the coasting portions of the extremals in Fig. 2 are likely to be optimal.

VII. Summary and Concluding Remarks

The characteristics of minimum-fuel, horizontal flight paths in the terminal area were investigated analytically and computationally. Analysis of the necessary conditions showed the following.

1) Thrust is continuous, but the bank angle may be switching for certain values of the velocity and heading costates λ_v and λ_ψ.

2) A straight-line segment may be fuel-optimal only if it is at the beginning of the flight path; a subsequent curved path, if any, must start by a switch to maximum bank angle while the thrust is at minimum value.

3) The optimal cruise velocity acts as an upper bound on the velocity for straight (or almost straight) minimum-fuel flight paths.

4) A circular flight path may be fuel-optimal only if both the bank angle and the velocity are at their respective constraint bounds.

The computation of extremals produced many representative minimum-fuel flight paths that can be categorized as long-range paths, short-range turning paths, and coasting (zero-thrust) paths. We found that:

1) Extreme sensitivity to the velocity costate for long-range paths could be overcome by starting integration at an appropriate intermediate state, rather than an end state.

2) Long-range paths with a large initial turn (over 100 deg) start by deceleration followed by an acceleration in the remainder of the turn.

3) Long-range paths with a final turn up to 140 deg end with zero thrust and turn with maximum bank-angle magnitude. However, if the final turn is large, and in particular if in addition to the final velocity $v(t_f)$ is higher than 180 knots, the turn is executed by decelerating below $v(t_f)$ and a final acceleration at maximum bank-angle magnitude. It is shown in Ref. 11 how these findings made possible the refinement of an existing on-line algorithm of Ref. 10 to the point where the fuel consumption of long-range, near-optimal paths is well within 1-3% that of optimal paths.

The near-optimal algorithm was very helpful also in alleviating the problem of finding the Darboux points. We found that:

1) Turning extremals that require thrust toward the end of the path, produced by backward integration from $v(t_f)=180$ knots, inevitably became nonoptimal at some point beyond $v=250$ knots.

2) Turning but coasting extremals, on the other hand, appear to be optimal no matter how long they were extended (backwards from a final velocity of $v(t_f)=180$ knots).

3) Optimality of long-range extremals may be lost if integration is extended so that the initial or final turns are much larger than 180 deg.

Evaluation of the optimality of extremals by a near-optimal algorithm proved to be a practical solution to the Darboux point question for flight-path problems. The general problem, however, is unresolved, for there is no test for Darboux points. Could a test for conjugate points (beyond which an extremal ceases to be *locally* optimal) be helpful? The answer appers to be negative; certainly so for a special two-dimensional case of the present problem, a line capture at constant velocity, which we examined in detail in Ref. 15. The question of global optimality, highlighted here by computation of extremals, is inherent (though perhaps less visible) in other optimization techniques. The problem of Darboux points remains a challenge for future research.

The work reported here is, of course, but one element in the development of a practical, fuel-efficient, and safe system for terminal operation. In particular, an extension to include the third dimension—altitude—is being studied.

Appendix A—Equations of Motion

The lateral, longitudinal, and vertical force equations are, respectively,

$$mv\dot{\psi} = -(L+T\sin\alpha)\sin\phi \tag{A1}$$

$$m\dot{v} = T\cos\alpha - D \tag{A2}$$

$$mg = (L+T\sin\alpha)\cos\phi \tag{A3}$$

For small angle-of-attack α, Eqs. (3) and (4) result, where $u=\tan\phi$.

Lift and drag are given by $L=C_{L_\alpha}\alpha qS$, $D=C_{D_0}qS+\epsilon L\alpha$, where ϵ is the efficiency factor and $q=(1/2)\rho v^2$ is the dynamic pressure, S the wing area, and the coefficients C_{L_α} and C_{D_0} are assumed to be independent of the velocity. Now,

$$\epsilon L\alpha = \epsilon L^2/(C_{L_\alpha}qS)\epsilon[mg/\cos\phi - T\sin\alpha]^2/(C_{L_\alpha}qS)$$

Neglecting $T\sin\alpha$, D is of the form of Eq. (5), with $k_1=(1/2)C_{D_0}\rho S$, $k_2=2\epsilon m^2g^2/(C_{L_\alpha}\rho S)$. Using the values $C_{D_0}=0.015$, $C_{L_\alpha}=0.08/\text{deg}$, $\epsilon=0.004/\text{deg}$, $(1/2)\rho=295^{-1}$ lb/ft^2/knot^2, $S=1560$ ft^2, $mg=150{,}000$ lb, gives the values of k_1 and k_2 in Sec. II.

Appendix B—Singular Case

When in Eq. (10) $c_2=0$, the thrust is a singular control. Here we derive the singular thrust and examine its optimality for various ranges of bank angle and velocity.

The Hamiltonian is now linear in T, with the term multiplying T given by

$$H_T = c_1 + \lambda_v/m \tag{B1}$$

Minimization of H with respect to T gives

$$T^* = \begin{cases} T_{\max} & \text{if } H_T<0 \\ T_{\min} & \text{if } H_T>0 \end{cases}$$

the thrust can be intermediate only in the singular case

$$H_T = 0 \quad \text{on a subinterval of} \quad [0,t_f] \tag{B2}$$

In this Appendix, we are concerned only with the case, Eq. (B2); therefore,

$$\lambda_v = -c_1 m \tag{B3}$$

Since in this Appendix λ_v is negative, minimization of H with respect to u yields

$$u^* = \begin{cases} gv\lambda_\psi/(2c_1k_2) & \text{if } |gv\lambda_\psi/(2c_1k_2)|<u_m \quad \text{(B4)} \\ u_m\,\text{sgn}\lambda_\psi & \text{if } |gv\lambda_\psi/(2c_1k_2)|\geq u_m \quad \text{(B5)} \end{cases}$$

The singular case, Eq. (B2), implies the vanishing of all time derivatives of H_T. Let the first time derivative of H_T in which T appears explicitly be the $2q$th (it is always even) where q is the order of the singular arc. The generalized Legendre-Clebsch necessary condition requires[16] that

$$(-1)^q[H_T^{(2q)}]_T \geq 0 \tag{B6}$$

Consider first the case $|u|<u_m$. Using Eqs. (16), (B3), and (B4) in $\dot{H}_T=0=\dot{\lambda}_v$, we compute $\ddot{H}_T$ to be

$$\ddot{H}_T = -g(\lambda_x\sin\psi - \lambda_y\cos\psi)u/mv - 2c_1(k_1v^4+3k_2)(T-D)/m^2v^4$$

First, we note that

$$(\ddot{H}_T)_T = -2c_1(k_1v^4+3k_2)/m^2v^4 < 0$$

so that the generalized Legendre-Clebsch necessary condition of Eq. (B5) is satisfied. Second, setting $\ddot{H}_T=0$ yields the intermediate, singular thrust

$$T = D - \frac{mgv(\lambda_x\sin\psi - \lambda_y\cos\psi)u}{2c_1(k_1v^2+3k_2/v^2)} \tag{B7}$$

Adding the condition $H=0$ to $H_T=\dot{H}_T=0$, we obtain

$$\lambda_\psi = \pm 2c_1\sqrt{k_2(3k_2 - k_1v^4 + c_0v^2/c_1)}/gv$$

and hence, using Eq. (B4),

$$u = \pm\sqrt{(3k_2 - k_1v^4 + c_0v^2/c_1)}/k_2 \tag{B8}$$

Using Eq. (B4), we find that the velocities for which $|u|<u_m$

are outside the range $[v_1, v_2]$, where v_1 and v_2 are the real and positive roots of

$$k_1 v^4 - c_0 v^2/c_1 + k_2(u_m^2 - 3) = 0 \tag{B9}$$

(Of course, real and positive v_1 or v_2, or both v_1 and v_2, may not exist; in particular, if $u_m^2 > 3$ and $(c_0/c_1)^2 < 4k_1k_2(u_m^2 - 3)$, then $|u| < u_m$ for all v.)

We observe that for a straight-line flight, setting $u = 0$ in Eq. (B7) gives $T = D$, which implies $v(t) = v_c = \text{const}$. Setting $u = 0$ in Eq. (B8), we obtain the optimal cruise velocity v_c^*

$$(v_c^*)^2 = c_0/(2k_1c_1) + [(c_0^2/(2k_1c_1)^2 + 3k_2/k_1]^{1/2} \tag{B10}$$

We now consider the case $|u| = u_m$, which occurs when the velocity enters the range $[v_1, v_2]$. Proceeding as in the previous case for $|u| < u_m$, we obtain

$$(\ddot{H}_T)_T = -3(c_1D - c_0)/(mv)^2 \tag{B11}$$

$$T = D - \frac{2mgv(\lambda_x \sin\psi - \lambda_y \cos\psi) u_m \operatorname{sgn}\lambda_\psi}{3(c_1D - c_0)} \tag{B12}$$

and

$$|\lambda_\psi| = c_1[3k_2(1 + u_m^2) - k_1v^4 + c_0v^2/c_1]/(2gvu_m)$$

We observe from Eq. (B11) that the generalized Legendre-Clebsch condition of Eq. (B5) is satisfied as long as

$$D = k_1v^2 + k_2(1 + u_m^2)/v^2 > c_0/c_1$$

or

$$k_1v^4 - c_0v^2/c_1 + k_1(1 + u_m^2) > 0 \tag{B13}$$

The left side of Eq. (B13) has no real zeros, and hence Eq. (19) holds if

$$c_0^2/(2c_1)^2 < k_1k_2(1 + u_m^2) \tag{B14}$$

If Eq. (B14) is violated (as when c_0 is increased to create a combined time and fuel cost functional), then there exists a range of velocities $[v_1', v_2']$, where v_1' and v_2' are the real and positive zeros of the left side of Eq. (B13), for which the singular thrust of Eq. (B12) is nonoptimal. We observe that $[v_1', v_2'] \subset [v_1, v_2]$, and, therefore, the generalized Legendre-Clebsch condition is satisfied whenever v is such that $|u| < u_m$.

We note that letting $u = u_m$, T in Eq. (B7) is different from that in Eq. (B12) (the author is indebted to Dr. H. Erzberger for this observation). This shows that the intermediate thrust is discontinuous at a time t_1, say, when the bank angle saturates. This is because $\ddot{H}_T$ contains $\dot{u}$ which is discontinuous at t_1 and so must be $T(t_1)$ in order to satisfy $\ddot{H}_T \equiv 0$.

We summarize this appendix as follows. For intermediate bank angle, the intermediate singular thrust is given by Eq. (B7) and it satisfies the generalized Legendre-Clebsch condition. The bank angle is given (except for sign) by Eq. (B8) and the velocity is outside the range $[v_1, v_2]$, with v_1 and v_2 being the real and positive roots of Eq. (B9). On a straight-line flight, the singular thrust is constant and the constant velocity is the optimal cruise velocity v_c^* given by Eq. (B10).

When the velocity enters the range $[v_1, v_2]$ the bank angle saturates $|u| = u_m$ and the intermediate singular thrust, now given by Eq. (B12), undergoes a jump. The singular thrust satisfies the generalized Legendre-Clebsch condition if Eq. (B14) holds; if Eq. (B14) does not hold, there exists a range of velocities $[v_1', v_2'] \subset [v_1, v_2]$, where v_1' and v_2' are the zeros of the left side of Eq. (B13), such that intermediate thrust is nonoptimal.

Acknowledgments

The authors wish to thank Dr. Heinz Erzberger for fruitful discussions and perceptive comments. This research was supported, for the first author, by a National Research Council Associateship at NASA Ames Research Center.

References

[1] Erzberger, H. and Lee, H.Q., "Optimum Horizontal Guidance Techniques for Aircraft," *Journal of Aircraft*, Vol. 8, Feb. 1971, pp. 95-101.

[2] Pecsvaradi, T., "Optimal Horizontal Guidance for Aircraft on the Terminal Area," *IEEE Transactions on Automatic Control*, Vol. AC-17, No. 6, Dec. 1972, pp. 763-772.

[3] Kishi, F.H. and Pfeffer, I., "Approach Guidance to Circular Flight Paths," *Journal of Aircraft*, Vol. 8, Feb. 1971, pp. 89-95.

[4] Hedrick, J.K. and Bryson Jr., A.E., "Minimum Time Turns for a Supersonic Airplane at Constant Altitude," *Journal of Aircraft*, Vol. 8, March 1971, pp. 182-187.

[5] Hoffman, W.C. and Bryson Jr., A.E., "Minimum Time Turns to a Specified Track," ASI-TR-71-4, Aerospace Systems, Inc., Sept. 1971; summarized in Hoffman, W.C., Zvara, J., and Bryson Jr., A.E., "Optimum Turns to a Specified Track for a Supersonic Aircraft," Preprints of Joint Automatic Control Conference, 1972, pp. 955-956.

[6] Bryson Jr., A.E. and Parson, M.G., "Constant Altitude Minimum Time Turns to a Line and to a Point for a Supersonic Aircraft with a Constraint on Maximum Velocity," SUDAAR No. 437, Stanford University, Stanford, Calif., Nov. 1971.

[7] Hoffman, W.C. and Bryson Jr., A.E., "Minimum Time Maneuvers to Specified Terminal Conditions," ASI-TR-73-12, Sec. 3.2, Aerospace Systems, Inc., Jan. 1973.

[8] Bryson Jr., A.E. and Lele, M.M., "Minimum Fuel Lateral Turns at Constant Altitude," *AIAA Journal*, Vol. 7, March 1969, pp. 559-560.

[9] Vinh, N.X., "Minimum Fuel Rocket Maneuvers in Horizontal Flight," *AIAA Journal*, Vol. 7, Feb. 1973, pp. 165-169.

[10] Erzberger, H. and McLean, J.D., "Fuel Conservative Guidance System for Powered Lift Aircraft," *Journal of Guidance and Control*, Vol. 4, No. 3, May/June 1981, pp. 253-261.

[11] Neuman, F. and Erzberger, H., "An Algorithm for Fuel Conservative Capture Trajectories," NASA TM 81334, Oct. 1981.

[12] Mereau, P.M. and Powers, W.F., "The Darboux Point," *Journal of Optimizaion Theory and Applications*, Vol. 17, Nos. 5/6, 1975, pp. 545-559.

[13] Jacobson, D.H., Lele, M.M., and Speyer, J.L., "New Necessary Conditions of Optimality for Control Problems with State-Variable Inequality Constraints," *Journal of Mathematical Analysis and Applications*, Vol. 35, 1971, pp. 255-284.

[14] Stern, T.E., *Theory of Non-Linear Networks and Systems. An Introduction*, Addison-Wesley, Reading, Mass., 1965.

[15] Kreindler, E. and Neuman, F., "Global Optimality of Extremals: An Example," *Journal of Optimization Theory and Applications*, Vol. 37, No. 4, Aug. 1982 (to appear); also NASA TM-81240, 1980.

[16] Bell, D.J. and Jacobson, D.H., *Singular Optimal Control Problems*, Academic Press, New York, 1975.